

Addressing Membership Inference Attack in Federated Learning with Model Compression

Gergely Dániel Németh
ELLIS Alicante
Alicante, Spain

gergely@ellisalicante.org

Miguel Ángel Lozano
University of Alicante
Alicante, Spain

malozano@ua.es

Novi Quadrianto
University of Sussex
Brighton, UK

n.quadrianto@sussex.ac.uk

Nuria Oliver
ELLIS Alicante
Alicante, Spain

nuria@ellisalicante.org

Abstract

Federated Learning (FL) has been proposed as a privacy-preserving solution for machine learning. However, recent works have shown that Federated Learning can leak private client data through membership attacks. In this paper, we show that the effectiveness of these attacks on the clients negatively correlates with the size of the client datasets and model complexity. Based on this finding, we propose model-agnostic Federated Learning as a privacy-enhancing solution because it enables the use of models of varying complexity in the clients. To this end, we present MaPP-FL, a novel privacy-aware FL approach that leverages model compression on the clients while keeping a full model on the server. We compare the performance of MaPP-FL against state-of-the-art model-agnostic FL methods on the CIFAR-10, CIFAR-100, and FEMNIST vision datasets. Our experiments show the effectiveness of MaPP-FL in preserving the clients' and the server's privacy while achieving competitive classification accuracies.

1. Introduction

Deep neural networks require access to large amounts of training data to achieve competitive performance. This data dependency raises concerns regarding the safeguarding of sensitive information that might be encapsulated in the data. Federated Learning (FL) has been proposed as a potential solution to mitigate such concerns [27]. FL consists of a distributed machine learning approach that enables training models without the need to transfer the raw data from different devices or locations (clients) to a central server. In each

iteration of the learning process, the server shares the parameters of the learned global model with the clients which perform local computations on their respective data to update their local parameters. Their updated model parameters are then sent back to the server, which aggregates the changes made by the clients to improve the global model.

Given that the raw data never leaves the clients and only the model parameters are shared with the central server, FL has been proposed as a privacy-preserving solution for machine learning [18]. It is particularly useful in scenarios where data is distributed across multiple devices or locations, and the data owners are reluctant to share their data due to privacy or security concerns, as it is the case in healthcare [23, 37] and finance [5, 26], or intelligent smartphone interfaces [2]. While FL aims to provide privacy-by-design by keeping the data private in the clients, recent work has shown that sensitive information about the original data can be inferred by analyzing the model parameters that are shared in the communication rounds [8, 12]. To tackle this limitation, several privacy-preserving approaches for FL have been proposed to date, including local differential privacy [3, 13] and data augmentation [19, 32].

In this paper, we analyze the privacy-performance trade-off in Federated Learning and propose model compression as an efficient strategy to increase the privacy of FL architectures. We present MaPP-FL, a novel approach to FL that achieves competitive accuracy while preserving privacy by leveraging a model-agnostic framework with heterogeneous clients. In model-agnostic FL, the models in the clients are not necessarily of the same type and complexity as the model in the server. Thus, it enables improving the learning efficiency and the inclusion in the federation of heterogeneous clients with different levels of computational [15, 24] and communication capabilities [7, 10, 25]. We compare

MaPP-FL’s performance with state-of-the-art methods on three benchmark vision datasets (CIFAR-10, CIFAR-100 and FEMNIST) and show its effectiveness in preserving both the clients’ and the server’s privacy while achieving competitive classification accuracies.

The rest of the paper is structured as follows: the most relevant prior work is presented in Sec. 2. Sec. 3 reports an analysis of the correlation between model complexity, dataset size and privacy and motivates the use of model-agnostic frameworks for preserving privacy in FL. Our proposed approach is described in Sec. 4. We empirically validate it and compare it with state-of-the-art methods in Sec. 5. Finally, we discuss our conclusions in Sec. 6.

2. Related work

Our work is related to both model-agnostic federated learning and privacy attacks and defenses in FL.

On membership attacks in FL: While FL was initially motivated by the desire to preserve client data, recent studies have revealed that federated systems remain vulnerable to privacy attacks, specifically in the form of membership attacks [3, 13, 19, 32]. In our work, we focus on Membership Inference Attacks (MIAs) [14], where the attacker’s goal is to determine whether an individual data point was part of the dataset used to train the target model. While MIAs expose less private information than other attacks, such as memorization attacks, they are still of great concern as they constitute a confidentiality violation [29]. Membership inference can also be used as a building block for mounting extraction attacks for existing machine learning as a service systems [8]. Several types of MIA have been proposed in the literature [17, 33, 34]. In this work, we focus on the loss-based attack by Yeom et al. [39], a light-weight attack where the attacker infers the data membership based on the loss of the data instance on the model based on a small number of known samples (attacker’s knowledge). This loss-based attack is one of the most efficient and widely used methods and it has been shown to perform similarly in terms of precision at low false positive rates than more complex attacks based on shadow models [9]. Section 3.1 describes Yeom attack in more detail.

On membership defenses in FL: Differential Privacy (DP) [11] has been proposed to protect models from membership attacks. One of the practical challenges of using DP is configuring the privacy parameters to strike a balance between privacy and utility. Existing analyses of privacy-preserving methods, such as DP-SGD [1] often rely on worst-case scenarios, and selecting privacy parameters solely based on theoretical results can result in a loss of utility. DP has also been found to yield significantly worse performance when training models on small datasets, such as the CIFAR-10 image dataset [19, 20]. Other methods to protect FL systems from membership attacks in-

clude applying a stronger data augmentation to configure the privacy-accuracy trade-off with the level of noise added through augmentation [19], and early stopping [36], given that membership memorization is partially caused by overfitting [39].

On model-agnostic FL: In horizontal FL, all clients use the same model architecture as the server. However, this approach can be a limitation when clients have different computational and communication capabilities. Model-agnostic FL has been proposed to address this limitation as it enables training a diversity of models in the clients according to their capacities. There are two broad types of model-agnostic FL methods: in the first category, clients leverage a public dataset to communicate via knowledge distillation, and learn completely different models without sharing a global model with the server [22, 40]. While this design lets clients train different model architectures without limitations, its disadvantage is the lack of a competitive model in the server. In the second category, clients learn a smaller version of the server’s models. In this case, both the server and client-side models are trained as part of the federation [7, 10, 25]. In the context of deep neural networks, the model compression on the clients side can be achieved with training models with fewer [25] or with simpler [7, 10, 15, 24] layers. Our work focuses on model-agnostic FL methods in this later category.

3. Privacy, dataset size and model complexity

Previous work has shown that as models get more complex, they are more vulnerable to membership attacks. For example, Yeom et al. [39] show that their attack’s accuracy increases as the model size increases on standard benchmark image datasets. In the case of FL with the same model size in the server and the clients (horizontal FL), Li et al. [23] perform model memorization attacks on ResNet networks of varying sizes and report that the larger the models, the more vulnerable they are to the attack. Similarly, over-parameterized models have been shown to be more vulnerable against membership memorization attacks in a FL setting [41]. In this section, we further study this and focus on the privacy-accuracy trade-off in FL with respect to dataset and model size, and from the perspective of both server and the clients. Prior studies have only analyzed server side performance.

3.1. Privacy attack using Yeom’s MIA model

We consider both client and server-side attacks: (1) *client* exposure or attack occurs when the attacker has access to the client’s parameters, θ_c^t , for client $c = 1, \dots, N$ in training round $t = 1, \dots, T$. In a stateful setting [28], the attacker can collect a set of $k \leq T$ client updates $\Theta_c = \{\theta_c^{t_1}, \dots, \theta_c^{t_k}\}$; (2) *server* exposure or attack takes place when the attacker is able to listen to the parameter

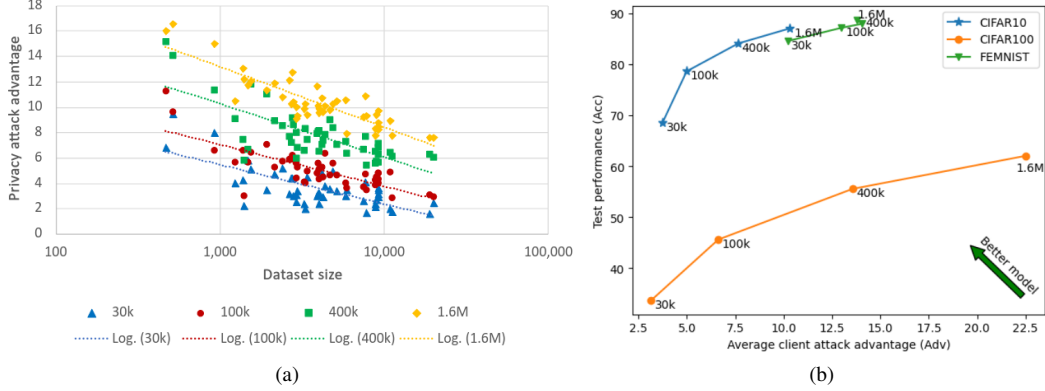


Figure 1. (a): Correlation between privacy attack advantage and dataset size from the clients’ perspective. Results for 5 repeated experiments on the CIFAR-10 dataset using the FedAvg architecture with 10 clients having different dataset sizes, resulting in 50 client models. Each dot depicts a client in one federated training and the color represents different model complexities (CNNs), characterized by the number of parameters, ranging from 30k to 1.6 million. Note the negative correlations between the size of the clients’ dataset and the attack advantage, as well as between the model’s complexity and the associated attack advantage. (b): Privacy-accuracy trade-off of the data depicted in (a) by averaging experiments across clients per model complexity. In addition to CIFAR-10, we also show the trade-off for the CIFAR-100 and FEMNIST datasets. The attacker’s advantage and test accuracy on the clients increases as the model size increases. Observations in (a) and (b) lead us to propose model-agnostic Federated Learning as a privacy-enhancing solution.

θ^t updates broadcasted by the server. Specifically, we assume *white-box, passive* attacks both at the server and client sides. In a white-box attack, the attacker has access to the model’s parameters θ_g and architecture f with the purpose of building an attacker model \mathcal{A} that predicts, for data instance (\mathbf{x}, y) , if it was part of the training data \mathbb{D}_g of model $M(f, \theta_g, \mathbb{D}_g)$, where the subscript g denotes both the server and each of the clients. Passive attackers do not modify their parameters during training to trick the other participants in the learning cycles to share their data.

Formally, the attacker model \mathcal{A} is given by:

$$\mathcal{A}(f, \theta_g, (\mathbf{x}, y)) = \begin{cases} 1, & \text{if } (\mathbf{x}, y) \in \mathbb{D}_g, M(f, \theta_g, \mathbb{D}_g) \\ 0, & \text{otherwise.} \end{cases} \quad (1)$$

In a server-side attack, the attack takes place on the last parameter update stored in the server $\theta_g = \theta^T$ and the attacker aims to identify the entire training dataset $\mathbb{D}_g = \mathbb{D} = \sum_c \mathbb{D}_c$. In the case of a client-side attack, we use the last update sent from the client to the server $\theta_g = \theta_c^T$ and the client’s dataset \mathbb{D}_c for client c .

In all our experiments, we use the loss-based *Yeom* attack of [39]. In this attack, the adversary has access to a subset of known data instances, called attacker’s knowledge: $\mathbb{D}_{\mathcal{A}+} \subset \mathbb{D}_g$ for samples from the training data and $\mathbb{D}_{\mathcal{A}-} \not\subset \mathbb{D}_g$. During the attack, the instance’s loss is compared with the average loss from the known training data points to infer the membership of data point (\mathbf{x}, y) to the

training dataset:

$$\mathcal{A}_{\text{Yeom}}(f, \theta, (\mathbf{x}, y)) = \begin{cases} 1, & \text{if } l(y, f(\mathbf{x}, \theta)) < \frac{1}{|\mathbb{D}_{\mathcal{A}+}|} \sum_{(\mathbf{x}', y') \in \mathbb{D}_{\mathcal{A}+}} l(y', f(\mathbf{x}', \theta)) \\ 0, & \text{otherwise.} \end{cases} \quad (2)$$

3.2. Privacy-accuracy trade-off w.r.t. dataset size

In this section, we empirically show that, for a given model and an FL scenario, there is a strong negative correlation between the size of the clients’ datasets and models, and their vulnerability against the *Yeom*’s attack. As previously discussed, this attack occurs on the last update the client sends to the server in round T , $\mathcal{A}_{\text{Yeom}}(\theta_c^T)$.

We perform the experiments on the CIFAR-10 image dataset (see Sec. 5 for a description of the dataset) with 10 clients and a FedAvg architecture for horizontal FL [27]. The idea behind FedAvg, summarized in Eq. (3), is that if the clients train the same model using their own dataset, the average of the clients’ model weights would be an approximation of training the same model in a centralized machine with access to all client data. That is, FedAvg computes: $\min_{\theta} L(\theta) =$

$$= \min_{\theta} \frac{1}{|\mathbb{D}|} \sum_{c=1}^C \sum_{(\mathbf{x}, y) \in \mathbb{D}_c} l(y, f(\mathbf{x}, \theta)) \approx \frac{1}{C} \sum_{c=1}^C \min_{\theta_c} L_c(\theta_c, \mathbb{D}_c) \quad (3)$$

where L is the loss function in the server when having access to all client data; l is the loss function in each client; θ

and f are server model parameters and server architecture, respectively. The loss at each client $L_c(\theta_c, \mathbb{D}_c)$ is given by $\frac{1}{|\mathbb{D}_c|} \sum_{(\mathbf{x}, y) \in \mathbb{D}_c} l(y, f(\mathbf{x}, \theta_c))$, where C is the number of clients; and \mathbb{D}_c represents the dataset of client c such that $\mathbb{D} = \bigcup_{c=1}^C \mathbb{D}_c$ corresponds to the entire dataset.

For a fair evaluation, the attacker’s knowledge dataset $\mathbb{D}_{\mathcal{A}+}$ for the Yeom’s attack is proportionate to the size of the training dataset. Specifically, we select 1%: $|\mathbb{D}_{\mathcal{A}+}| = 0.01|\mathbb{D}|$ for the server-side attack and $|\mathbb{D}_{\mathcal{A}+}| = \min(3, 0.01|\mathbb{D}_c|)$ for the attack on client c . The MIA test dataset $|\mathbb{D}_{\text{MIA}}|$ includes the same number of samples from the training set as samples from outside of the training set. For the server-side attack, the MIA test data contains 5,000 samples from the training dataset \mathbb{D} and the same from the test dataset \mathbb{D}_{test} . If the client c has less than 5,000 data samples, the partition sampled from the test set is reduced accordingly, that is $|\mathbb{D}_{\text{MIA}}| = 2\mathbb{D}_c$. With such a dataset setting, a simple baseline which guesses that each MIA test data point is part of the training dataset would give a 50% accuracy. We define the **attack advantage** [16] as the improvement of an attack when compared to this baseline according to:

$$Adv(\mathcal{A}) = 2(Acc(\mathcal{A}) - 50). \quad (4)$$

In all the experiments we adopt the model architecture proposed in [10]. It consists of a convolutional neural network (CNN) with 4 convolutional layers and one fully connected layer at the end. We adjust the model complexity by changing the number of channels in the convolutional layers and the number of units in the last fully connected layer. We define 4 levels of model complexity and train 5 models for each level of complexity using FedAvg with class-balanced data in each client, resulting in 50 client models. The complexity of the models is measured by the number of parameters, ranging from models with 30k parameters to models with 1.6 million parameters.

For each model complexity, we compute the Pearson correlation coefficient between the logarithm of the clients’ dataset size, $\log_{10}(|\mathbb{D}_c|)$, and the attack advantage on the clients’ final update, $Adv(\mathcal{A}_{\text{Yeom}}(\theta_c^T))$. Fig. 1(a) visually illustrates the correlation between the client dataset size and the attack advantage on CNN models of increasing complexity on the CIFAR-10 dataset. Note that clients with less than 400 data points are not considered in the calculation as their attack performance is not consistent through runs due to having very small (< 4) attacker knowledge. Fig. 1(b) shows the privacy-accuracy trade-off by averaging experiments across clients for each model complexity on the CIFAR-10, CIFAR-100, and FEMNIST datasets. We observe strong negative correlations between the size of the clients’ dataset and the attack advantage; and between the clients’ model complexity and the corresponding attack advantage. We also observe that the attacker’s advantage and test accuracy on the clients increase as the model size in-

Dynamic client size selection methods		
	Random	Gradient
Update Each round		Flado [24]
Update Each batch	FjORD [15]	

(a) FL methods with dynamic selection of the clients’ model size. All clients are assumed to hold a model of the same complexity as the server’s model. These methods are not applicable to our setting where clients have data and computation constraints. Thus, they are beyond the scope of this paper.

Selection strategy		
	Resampled (S)	Fixed (F)
Coverage One group (O)		HeteroFL [10]
Coverage Several groups (G)		MaPP-FL (ours)
Coverage Unique (U)	FDropout [7]	

(b) FL channel selection methods with fixed model size in the clients. Clients are allowed to learn simpler (smaller) models than the server’s model. Empty cells in the Table will be analysed in Sec. 5.4.

Table 1. Taxonomy of proposed methods to achieve model-agnostic FL by means of model compression in the clients.

creases.

4. MaPP-FL

Motivated by the previous analysis, we present MaPP-FL, a model-agnostic approach to FL that preserves privacy both in the server and the clients while maintaining competitive accuracies.

4.1. Formulation

In the following, we assume a model-agnostic FL architecture where both the server and clients’ models are CNNs with a different number of channels in each layer, but the same number of layers.

In this setting, a model-agnostic FL method achieves model reduction $\theta_c \subset \theta$ in client c by limiting the size of each layer in the client’s network according to the following principle: a layer represented by weight matrix $\mathbf{A}^{N \times M} \in \theta$ is reduced to size $N_c \times M_c$, where $N_c < N$ and $M_c < M$ such that every cell $a_c^{i_c, j_c}$ the reduced matrix $\mathbf{A}_c^{N_c \times M_c}$ corresponds to a cell $a^{i, j}$ in the original matrix $\mathbf{A}^{N \times M}$:

$$\forall i_c, j_c : a_c^{i_c, j_c} \in \mathbf{A}_c, \exists i, j : a^{i, j} \in \mathbf{A}, a_c^{i_c, j_c} = a^{i, j}. \quad (5)$$

To present an overview of how our model-agnostic Federated Learning compares to existing approaches, we introduce a taxonomy of model-agnostic FL methods in Tab. 1. The first group of methods shown in Tab. 1 (a) includes algorithms that *dynamically* select the size of the clients’ models but where all the clients hold models of the same complexity as the server. Formally, these methods define an $Ms(\cdot)$ function that determines the $N_c^l \times M_c^l$ dimensions of the weight matrix \mathbf{A}_c^l for each layer l in the model $f(\theta_c)$ of client c . Note that the methods in this category assume that

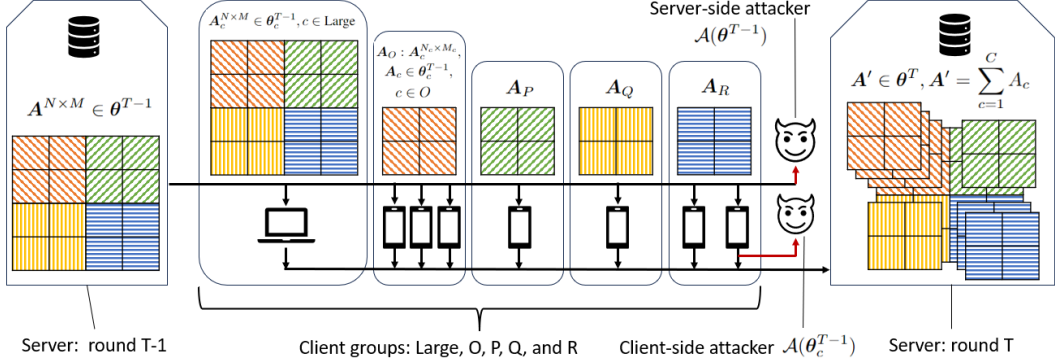


Figure 2. Illustration of MaPP-FL. The server and the clients learn models of the same family (CNNs) but with different complexities (reflected by the size of the weight matrix A). In round $T - 1$, the server shares the updated values of the weights to the clients. The clients perform local computations with the new weights and send back their updates. The server aggregates the received weights in round T . Server-side and client-side attackers are represented with a demon icon.

all the clients are able to have models of size $N \times M$, but only a subset of the dimensions are selected in each round of training. Flado [24] and FjORD [15] are under this first group.

The second group depicted in Tab. 1 (b) includes methods where the clients have *fixed-size* models that are typically smaller than the server’s model. As the most prevalent type of models to perform image classification tasks are CNNs, we refer to this family of methods as *channel selection* methods.

The weights of each layer in a 2D convolutional network are defined by an (N, M, H, W) dimensional tensor, where M and N are the input and output channels of the layer and H and W are the height and width of the kernel. For each linear layer, $A^{N \times M}$ denotes its weight matrix where M and N are the input and output data dimensions [21, 42], and $a^{i,j}$ represents the kernel weights of the given position. In this case, $Ch(\cdot) : A^{N \times M} \rightarrow A_c^{N_c \times M_c}$ determines the mapping between the cells of the server’s weight matrix A^l and client’s c smaller matrix A_c^l for each layer l . Without a loss of generalization, we assume that the channels are sorted, thus if channel i was before channel j in the server, their order is the same in the client.

According to this taxonomy of model-agnostic FL, Federated Dropout (FDropout) [7] and HeteroFL [10] belong to the same group of approaches as the proposed MaPP-FL. Next, we present the channel selection strategies adopted by each of these methods.

4.2. Channel selection algorithms

As shown in Tab. 1(b), FDropout, HeteroFL and MaPP-FL belong to the same family of methods with differences that can be characterized in two ways. First, according to the number of clients selecting the same channels: in HeteroFL, all clients with the same model size select the same channels in the server’s weight matrix in

each layer of the network; MaPP-FL creates groups of clients; and in FDropout each client has its own set of unique channels. Second, according to the method used to select the channels in each group of clients: FDropout randomly selects the channels in each round of training whereas HeteroFL and MaPP-FL determine the channels at the beginning of the training. We describe next each of these approaches in more detail and for the case of CNNs.

4.2.1 Channel selection in FDropout and HeteroFL

In FDropout [7], all the clients learn a CNN with the same architecture but fewer parameters (smaller weight matrices) as the server, and the server randomly drops a fixed number of units from each client [35], mapping the sparse model to a dense, smaller network by removing the dropped weights ("Unique" row in Tab. 1 (b)).

While the original formulation of FDropout used the same model size in all the clients, an extended model-agnostic variation was proposed by [15] that allows clients to have different model sizes. In this variation, randomly selected cells, $a^{i,j}$ and their associated rows i and columns j are dropped from the weight matrix. The size of the client’s matrix can be set by the number of dropped rows and columns: $|Drop(N, N_c)| = N - N_c$ and $|Drop(M, M_c)| = M - M_c$, where $Drop(n, k)$ selects k elements from n randomly. Therefore, for FDropout, we have:

$$a^{i,j} \in A_c : i \notin Drop(N, N_c), j \notin Drop(M, M_c). \quad (6)$$

HeteroFL [10] follows a similar idea as FDropout but with two key differences: 1) instead of randomly dropping cells, the clients always keep the top-left subset of the server’s weight matrix for each layer in the network ("One group" in Tab. 1 (b)); and 2) the clients learn networks with the same number of layers but with different –smaller than the server– number of channels.

Thus, in `HeteroFL`, the weight matrix \mathbf{A}_c^l of size $N_c \times M_c$ in layer l and client c corresponds to the top-left sub-matrix of the server's weight matrix \mathbf{A}^l of size $N \times M$:

$$\forall a_c^{i,j} \in \mathbf{A}_c, a^{i,j} \in \mathbf{A} : a_c^{i,j} = a^{i,j}, i = 1..N_c, j = 1..M_c. \quad (7)$$

`HeteroFL` has been reported to achieve a similar performance to horizontal FL but with only a portion of the clients having learned a network as large as the server's model [10].

Note that while both `HeteroFL` and `FDropout` are explained using the weight matrix of a layer in the model independently from other layers, in practice the input channels of layer l must be the same as the output channels of the previous layer ($l-1$) in sequential models. The `FDropout` implementation in [24] follows the same principle. Therefore, the input channels –columns of the weight matrix \mathbf{A} – are inherited from the previous layer in the network, and only the output channels –rows of the weight matrix– are selected for the current layer.

4.2.2 Channel selection in MaPP-FL

The proposed `MaPP-FL` method may be considered to be a generalization of `HeteroFL`: instead of selecting the top-left sub-matrix of the server's model, the clients are randomly placed in N groups. In the following, we present the example where $N = 4$. Thus, the clients are assigned to one of 4 groups, O, P, Q, R with their corresponding groups of channels or sub-matrices, such that each cell from the original matrix is assigned to one cell in one of the four group sub-matrices.

`MaPP-FL`'s approach to channel selection is illustrated in Fig. 2.

The matrix assigned to group O is the same as the `HeteroFL` sub-matrix: it always selects the top-left cells of the server's matrix. Clients in group R are assigned the bottom-right cells, while the sub-matrices assigned to clients in groups O and P alternate between the bottom-left and the top-right cells. This is due to the restriction on the input-output channels. The top-right sub-matrix corresponds to selecting the second half of the input channels and the first half of the output channels. Therefore, if in layer l the client selected the top-right sub-matrix, in the next layer it has to select one of the left sub-matrices, as they are the ones with the first half of the input channels. Note that this approach can be generalized to 9, 16,... groups, depending on the number of clients and the desired model size reduction. The cell assignment in the sub-matrices of each of the

four groups can be summarised as:

$$a^{(i,j),l} \in \begin{cases} \mathbf{A}_O, & \text{if } 1 \leq i \leq N_c, 1 \leq j \leq M_c \\ \mathbf{A}_P, & \text{if } 1 \leq i \leq N_c, M - M_c \leq j \leq M, l \text{ odd,} \\ & \text{or } N - N_c \leq i \leq N, 1 \leq j \leq M_c, l \text{ even} \\ \mathbf{A}_Q, & \text{if } N - N_c \leq i \leq N, 1 \leq j \leq M_c, l \text{ odd,} \\ & \text{or } 1 \leq i \leq N_c, M - M_c \leq j \leq M, l \text{ even} \\ \mathbf{A}_R, & \text{if } N - N_c \leq i \leq N, M - M_c \leq j \leq M \end{cases} \quad (8)$$

Our design of `MaPP-FL` draws inspiration from both `FDropout` for its effective privacy protection through randomness and `HeteroFL` for its strong performance resulting from structural considerations. We expect `HeteroFL` to have worse privacy because parts of the aggregated model are only trained by the large clients due to its strict structure or channel grouping. We expect `FDropout` to have more privacy protection but worse performance as the channels are selected randomly, without following a particular structure or channel grouping. The experimental results reported in Sec. 5 corroborate these expectations.

5. Experiments

Here, we report our experimental evaluation of `MaPP-FL` and related baselines in terms of both server and client accuracy and privacy.

5.1. Datasets

We perform experiments on three widely used image datasets: CIFAR-10, CIFAR-100 and FEMNIST.

CIFAR-10 [20] is a commonly used dataset both in the FL [10, 15, 27] and the membership inference attacks [19, 39] literature. It contains 60,000 images from 10 classes (50,000 images for training and validation and 10,000 images for testing).

CIFAR-100 [20] has the same number of training and testing images as CIFAR-10 but with 100 classes and 500 training images per class.

Both in the CIFAR-10 and CIFAR-100 datasets, we distribute the training images among all the clients, and use the entire test dataset for testing the models both on the server and the clients.

Federated EMNIST or FEMNIST [6] is an image dataset of hand-written character digits derived from the NIST Special Database 19 and converted to a 28x28 pixel image format. It consists of 62 classes with a long-tail data distribution such that some of the writers can have samples from as few as 10 classes. In its federated version, the images are distributed by the ID of the writer whose handwriting they are. Following the official sub-sampling method, we select 20% of the data, keeping only writers with at least 300 samples and splitting into train-test datasets where the test dataset corresponds to images by unseen. This results in approximately 165 writers in the train set. We distribute

the data among clients following the standard practice in the literature [38]. We use this dataset to study the performance of the models on non-IID (non independent and identically distributed) data.

For the CIFAR-10 and CIFAR-100 datasets, we use a class-wise balanced, but client-wise weighted-distribution. We generate a data distribution using the Dirichlet distribution $Dir(\alpha)$ once, and apply the same split for each class. This ensures that each client has the same number of images from each class while they have different dataset sizes. The IID-ness of the data is controlled by the $\alpha \in (0, \infty)$ value of the Dirichlet distribution: the larger the α , the closer the allocation of training data to the uniform distribution and hence the closer to an IID scenario. Using $\alpha = 0.85$ this distribution generates clients with dataset size typically ranging from 1,000 to 10,000 samples.

5.2. Methodology

Machine learning (ML) model. Given the nature of the data (images), we use a sequential CNN architecture, with convolutional, static batch normalization and fully connected layers with trainable weights following [10]. Appendix 7 describes the model architecture in detail. We control the model complexity by changing the number of channels in convolutional layers and the number of units in the final fully connected layer. In our experiments, we increase the complexity by factors of 2: each increase in the level of model complexity means doubling the input and output channel sizes in each inner convolutional layer and the number of units in the final fully connected layer.

Experimental setup. In all experiments we define a FL architecture with 10 clients which are trained with the Adam optimizer, a learning rate of 0.001 for one local epoch, a batch size of 128, and 150 rounds of FL. Experiments are repeated 3 times and we report mean values. The server learns a *large* model, which corresponds to a CNN network with 100k parameters. The clients learn a model with either the same complexity as the server’s model or one complexity level below with 30k parameters (*small* model).

In terms of implementation, all models are built in PyTorch [30] and the FL methods are implemented in the Flower federated framework [4]. Our code is available at <https://github.com/negedng/ma-fl-mia>

5.3. Model-agnostic FL evaluation

We first perform experiments to evaluate the performance of MaPP-FL when compared to other SOTA methods.

In this first set of experiments, we have a class-balanced data distribution, where the clients have an increasing portion of the datasets controlled by $Dir(\alpha = 0.85)$. We simulate 10 privacy-aware clients that decide to opt into the federation with either a large or a small model. The number of channels in the small model is half the number in the large models.

As a solution to solve the disparity of motivations of different actors, we propose to use model-agnostic training. We compare MaPP-FL with 3 baselines: 1) all participating clients learn large models using FedAvg; 2) all participating clients learn small models using FedAvg; 3) the clients with small models refuse to participate and thus train a local model (Local). We train FL architectures ranging from 1 to 9 clients learning large models.

As an example, Tab. 2 illustrates the results with a model-agnostic setup where 2 clients learn large models and the remaining 8 clients learn small models. The top part of the table reflects client-side results, where each row corresponds to one client with dataset size shown in the left-most column. The bottom part of the table corresponds to the server’s perspective. Training is repeated 3 times with the same dataset size distribution, but images are reshuffled between runs.

From the server’s perspective, the highest accuracy but largest privacy vulnerability is reached with FedAvg where all the clients learn large models. The privacy advantage is halved when learning a small model using FedAvg, but at the cost of a ≈ 10 point decrease in accuracy. Learning in a model with MaPP-FL significantly improves its defense against privacy attacks on the server model while maintaining competitive levels of accuracy.

From the clients’ perspective, small clients are motivated to participate in the MaPP-FL federation as the client models learned with MaPP-FL outperform those learned locally (Local) by 13.5% on average.

Dataset size	Client side performance							
	FedAvg(100k)		FedAvg(30k)		Local		MaPP-FL(44k)	
Acc \uparrow	Adv \downarrow	Acc \uparrow	Adv \downarrow	Acc \uparrow	Adv \downarrow	Acc \uparrow	Adv \downarrow	
17020	78.2	2.82	68.57	0.66	-	-	77.14	4.42
7400	78.2	3.48	68.57	1.86	-	-	77.14	4.02
7040	78.2	3.44	68.57	1.44	61.57	-	66.3	1.52
6310	78.2	3.78	68.57	2.14	59.12	-	63.95	2.04
4060	78.2	4.66	68.57	2.73	55.29	-	66.3	2.81
3110	78.2	3.57	68.57	2.12	53.91	-	65.84	0.35
1660	78.2	5.48	68.57	6.69	50.49	-	66.3	6.33
1650	78.2	6.67	68.57	5.94	51.62	-	65.84	1.52
1260	78.2	3.97	68.57	4.21	49.74	-	68.48	1.75
490	78.2	9.8	68.57	5.31	41.53	-	68.48	5.92
Server side performance								
50000	78.29	2.26	68.73	1.16	-	-	76.54	1.42

Table 2. MaPP-FL (clients and server) performance in a federation with 10 clients, of which 2 clients learn models of the same complexity as the server’s model (100k params) and the rest of the clients learn smaller models (30k params). Client side test accuracy of the last weight update received by the clients and attack advantage on the last weight update sent by the clients. Server side results after last client update. Note how the performance of the client models learned with MaPP-FL is significantly better than if they trained their models locally. The server’s performance is also significantly better than in FedAvg with models of 30k parameters.

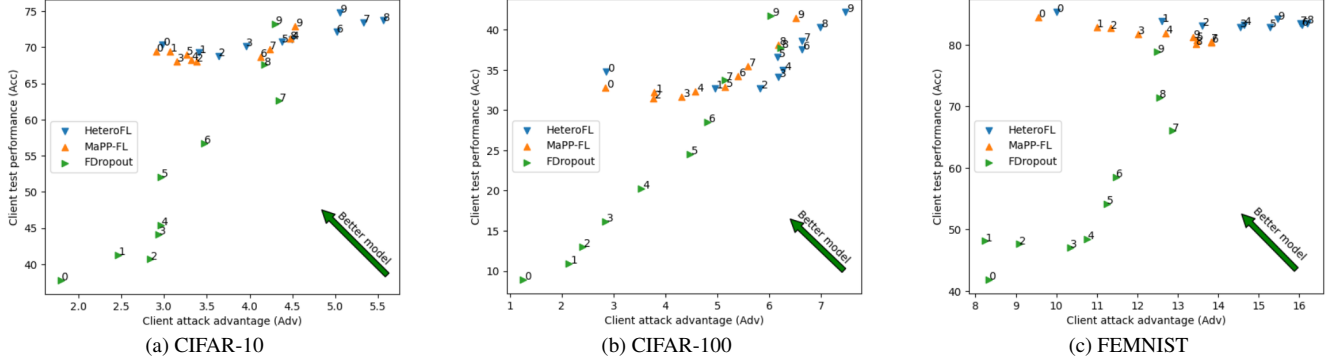


Figure 3. Client accuracy vs attack advantage in the CIFAR-10, CIFAR-100 and FEMNIST datasets for different model-agnostic FL architectures with 10 clients. Each symbol denotes a different FL method. The number next to each symbol indicates the number of large clients in the federation. The results correspond to the average values after running each experiment three times. Our results show that MaPP-FL models have the best accuracy-privacy trade-off across datasets.

Next, we compare the performance on the CIFAR-10, CIFAR-100, and FEMNIST datasets of FDropout, HeteroFL and MaPP-FL in a FL architecture with 10 clients, varying the number of large clients in the federation from 1 to 9. Fig. 3 shows the average client accuracy and attack advantage. Client models learned with MaPP-FL have the **best accuracy-privacy** trade-off: they achieve both competitive levels of privacy –similar to those obtained with FDropout– and accuracy –similar to HeteroFL’s. All model-agnostic methods achieve similar performance on the server side model, which is competitive with FedAvg. See Appendix 8 for details.

5.4. Ablation study of the variations of MaPP-FL

Following the taxonomy of Tab. 1 (b), we design variations of the MaPP-FL algorithm family to test all possible combinations of coverage and channel selection methods. The results on the CIFAR-10 dataset are depicted in Figure 4.

Regarding the strategy for channel selection, we define: *fixed* (F) methods when the channel sets are defined at the beginning of the training, and *resampled* (S) methods when the channel sets are selected in each training round. Furthermore, *submatrix* (M) methods if the selected channels are the first or second half of the full channel list and *random* (R) methods if the channels are selected randomly.

With respect to coverage, we classify the methods in three classes: *one group* (O); *several groups* (G); and *unique* (U), depending on the number of different channel sets the clients train on.

Following this convention, HeteroFL can be identified as OFM in the Figure: there is one group of small clients (O), the channel sets are defined at the beginning of the training (F) and it always selects the first, top-left submatrix of the weight matrix (M). HeteroFL (R) is the variation of HeteroFL where the small clients’ channels are a random set of $N/2$ elements of the $\{1, \dots, N\}$ in the server.

Similarly, MaPP-FL is represented as GFM in the Figure: it defines groups (G) of disjoint matrices (M) and the channel sets are defined at the beginning of the training (F). The MaPP-FL (R) variation defines the 4 sets of channels for the groups at the beginning of the training randomly. In the Figure, the original version is denoted by MaPP-FL (M).

With this taxonomy FDropout is identified as USR: each small client has a unique (U) set of channels drawn randomly (R) in each round (S). Additional methods include OSR and GSR, when random (R) sets of channels are drawn in each round (S) for one (O) or several groups (G) of clients; OSM, when one (O) of disjoint matrices (M) is selected randomly for each client in each round (S); and UFR, a unique (U) C set of channels is defined at the beginning of the training (F) and the clients select one at random (R) in each round without replacement.

The results reported in Figure 4 correspond to experiments that are repeated 3 times in a federation with 2 large clients in a class-balanced data distribution setting. The Figure shows the average client side accuracy-privacy trade-off for all the previously described variations of model-agnostic FL methods.

As shown in the Figure, MaPP-FL achieves the best accuracy-privacy trade-off: it balances the effective privacy protection of FDropout through randomness and the strong performance of HeteroFL through structural considerations.

6. Conclusion

We have proposed MaPP-FL, a novel model-agnostic FL method with significantly better client privacy-performance trade-off than current SOTA approaches. We have empirically shown that model compression is effective in enhancing the privacy of the clients and we have also proposed a taxonomy that unifies previously defined model-agnostic

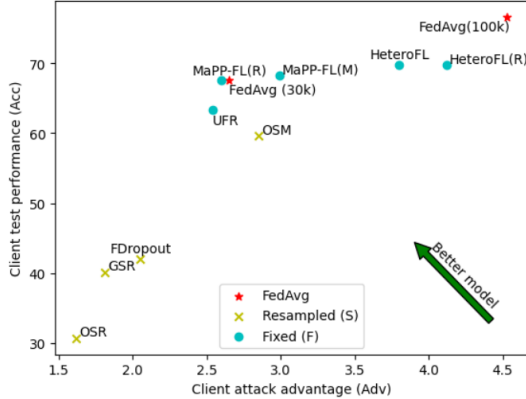


Figure 4. Ablation study: client accuracy vs attack advantage for variations of channel selection methods on the CIFAR-10 dataset with a federation of 10 clients, of which 2 learn large models. All experiments are repeated 3 times with images redistributed among the clients with a defined dataset size between repeats. Note how the larger the randomness (S and R methods), the worse the privacy-performance trade-off.

FL methods. In future work, we plan to investigate the interplay between MaPP-FL and fair client allocations [31].

Acknowledgement

G.D.N. and N.O. have been partially supported by funding received at the ELLIS Unit Alicante Foundation by the European Commission under the Horizon Europe Programme - Grant Agreement 101120237 - ELIAS, and a nominal grant from the Regional Government of Valencia in Spain (Convenio Singular signed with Generalitat Valenciana, Conselleria de Innovación, Industria, Comercio y Turismo, Dirección General de Innovación). G.D.N. is also funded by a grant by the Banco Sabadell Foundation. G.D.N and N.Q. have been supported in part by a European Research Council (ERC) Starting Grant for the project “Bayesian Models and Algorithms for Fairness and Transparency”, funded under the European Union’s Horizon 2020 Framework Programme (Grant Agreement 851538).

References

- [1] Martin Abadi, Andy Chu, Ian Goodfellow, H. Brendan McMahan, Ilya Mironov, Kunal Talwar, and Li Zhang. Deep learning with differential privacy. In *Proceedings of the 2016 ACM SIGSAC conference on computer and communications security*, page 308–318, New York, NY, USA, 2016. Association for Computing Machinery. [2](#)
- [2] KS Arikumar, Sahaya Beni Prathiba, Mamoun Alazab, Thippa Reddy Gadekallu, Sharnil Pandya, Javed Masood Khan, and Rajalakshmi Shenbaga Moorthy. Fl-pmi: Federated learning-based person movement identification through wearable devices in smart healthcare systems. *Sensors*, 22(4):1377, 2022. [1](#)
- [3] Daniel Bernau, Jonas Robl, Philip W Grassal, Steffen Schneider, and Florian Kerschbaum. Comparing local and central differential privacy using membership inference attacks. In *Data and Applications Security and Privacy XXXV: 35th Annual IFIP WG 11.3 Conference, DBSec 2021, Calgary, Canada, July 19–20, 2021, Proceedings*, pages 22–42. Springer, 2021. [1, 2](#)
- [4] Daniel J Beutel, Taner Topal, Akhil Mathur, Xinchi Qiu, Javier Fernandez-Marques, Yan Gao, Lorenzo Sani, Hei Li Kwing, Titouan Parcollet, Pedro PB de Gusmão, and Nicholas D Lane. Flower: A friendly federated learning research framework. *arXiv preprint arXiv:2007.14390*, 2020. [7](#)
- [5] David Byrd and Antigoni Polychroniadou. Differentially private secure multi-party computation for federated learning in financial applications. In *Proceedings of the First ACM International Conference on AI in Finance*, pages 1–9, 2020. [1](#)
- [6] Sebastian Caldas, Sai Meher Karthik Duddu, Peter Wu, Tian Li, Jakub Konečný, H. Brendan McMahan, Virginia Smith, and Ameet Talwalkar. Leaf: A benchmark for federated settings. *arXiv preprint arXiv:1812.01097*, 2018. [6](#)
- [7] Sebastian Caldas, Jakub Konečný, H. Brendan McMahan, and Ameet Talwalkar. Expanding the reach of federated learning by reducing client resource requirements, 2018. [1, 2, 4, 5](#)
- [8] Nicholas Carlini, Chang Liu, Úlfar Erlingsson, Jernej Kos, and Dawn Song. The secret sharer: Evaluating and testing unintended memorization in neural networks. In *USENIX Security Symposium*, 2019. [1, 2](#)
- [9] Nicholas Carlini, Steve Chien, Milad Nasr, Shuang Song, Andreas Terzis, and Florian Tramèr. Membership inference attacks from first principles. In *2022 IEEE symposium on security and privacy (SP)*, pages 1897–1914. IEEE, 2022. [2](#)
- [10] Enmao Diao, Jie Ding, and Vahid Tarokh. Hetero{fl}: Computation and communication efficient federated learning for heterogeneous clients. In *International Conference on Learning Representations*, 2021. [1, 2, 4, 5, 6, 7](#)
- [11] Cynthia Dwork. Differential privacy. In *International colloquium on automata, languages, and programming*, pages 1–12. Springer, 2006. [2](#)
- [12] Matt Fredrikson, Somesh Jha, and Thomas Ristenpart. Model inversion attacks that exploit confidence information and basic countermeasures. In *Proceedings of the 22nd ACM SIGSAC conference on computer and communications security*, pages 1322–1333, 2015. [1](#)
- [13] Yuhao Gu, Yuebin Bai, and Shubin Xu. Cs-mia: Membership inference attack based on prediction confidence series in federated learning. *Journal of Information Security and Applications*, 67:103201, 2022. [1, 2](#)
- [14] Nils Homer, Szabolcs Szalinger, Margot Redman, David Duggan, Waibhav Tembe, Jill Muehling, John V. Pearson, Dietrich A. Stephan, Stanley F. Nelson, and David W. Craig. Resolving individuals contributing trace amounts of dna to highly complex mixtures using high-density snp genotyping microarrays. *PLOS Genetics*, 4:1–9, 2008. [2](#)
- [15] Samuel Horvath, Stefanos Laskaridis, Mario Almeida, Ilias Leontiadis, Stylianos Venieris, and Nicholas Lane. Fjord:

Fair and accurate federated learning under heterogeneous targets with ordered dropout. *Advances in Neural Information Processing Systems*, 34:12876–12889, 2021. 1, 2, 4, 5, 6

[16] Hongsheng Hu, Zoran Salcic, Lichao Sun, Gillian Dobbie, Philip S Yu, and Xuyun Zhang. Membership inference attacks on machine learning: A survey. *ACM Computing Surveys (CSUR)*, 54(11s):1–37, 2022. 4

[17] Bargav Jayaraman, Lingxiao Wang, Katherine Knipmeyer, Quanquan Gu, and David Evans. Revisiting membership inference under realistic assumptions. *Proceedings on Privacy Enhancing Technologies*, 2021(2), 2021. 2

[18] Peter Kairouz, H. Brendan McMahan, Brendan Avent, Aurélien Bellet, Mehdi Bennis, Arjun Nitin Bhagoji, Kallista Bonawitz, Zachary Charles, Graham Cormode, Rachel Cummings, Rafael G. L. D’Oliveira, Hubert Eichner, Salim El Rouayheb, David Evans, Josh Gardner, Zachary Garrett, Adrià Gascón, Badih Ghazi, Phillip B. Gibbons, Marco Gruteser, Zaid Harchaoui, Chaoyang He, Lie He, Zhouyuan Huo, Ben Hutchinson, Justin Hsu, Martin Jaggi, Tara Javidi, Gauri Joshi, Mikhail Khodak, Jakub Konecný, Aleksandra Korolova, Farinaz Koushanfar, Sanmi Koyejo, Tancrede Le-point, Yang Liu, Prateek Mittal, Mehryar Mohri, Richard Nock, Ayfer Özgür, Rasmus Pagh, Hang Qi, Daniel Ramage, Ramesh Raskar, Mariana Raykova, Dawn Song, Weikang Song, Sebastian U. Stich, Ziteng Sun, Ananda Theertha Suresh, Florian Tramèr, Praneeth Vepakomma, Jianyu Wang, Li Xiong, Zheng Xu, Qiang Yang, Felix X. Yu, Han Yu, and Sen Zhao. Advances and open problems in federated learning. *Foundations and Trends® in Machine Learning*, 14(1–2):1–210, 2021. 1

[19] Yigitcan Kaya and Tudor Dumitras. When does data augmentation help with membership inference attacks? In *Proceedings of the 38th International Conference on Machine Learning*, pages 5345–5355. PMLR, 2021. 1, 2, 6

[20] Alex Krizhevsky. Learning multiple layers of features from tiny images. Master’s thesis, University of Tront, 2009. 2, 6

[21] Yann LeCun, Bernhard Boser, John S Denker, Donnie Henderson, Richard E Howard, Wayne Hubbard, and Lawrence D Jackel. Backpropagation applied to handwritten zip code recognition. *Neural computation*, 1(4):541–551, 1989. 5

[22] Daliang Li and Junpu Wang. Fedmd: Heterogenous federated learning via model distillation. *arXiv preprint arXiv:1910.03581*, 2019. 2

[23] Zhaohua Li, Le Wang, Guangyao Chen, Zhiqiang Zhang, Muhammad Shafiq, and Zhaoquan Gu. E2egi: End-to-end gradient inversion in federated learning. *IEEE Journal of Biomedical and Health Informatics*, 2022. 1, 2

[24] Dongping Liao, Xitong Gao, Yiren Zhao, and Cheng-Zhong Xu. Adaptive channel sparsity for federated learning under system heterogeneity. In *Proceedings of the IEEE/CVF Conference on Computer Vision and Pattern Recognition*, pages 20432–20441, 2023. 1, 2, 4, 5, 6

[25] Ruixuan Liu, Fangzhao Wu, Chuhan Wu, Yanlin Wang, Lingjuan Lyu, Hong Chen, and Xing Xie. No one left behind: Inclusive federated learning over heterogeneous devices. In *Proceedings of the 28th ACM SIGKDD Conference on Knowledge Discovery and Data Mining*, pages 3398–3406, 2022. 1, 2

[26] Guodong Long, Yue Tan, Jing Jiang, and Chengqi Zhang. Federated learning for open banking. In *Federated Learning: Privacy and Incentive*, pages 240–254. Springer, 2020. 1

[27] Brendan McMahan, Eider Moore, Daniel Ramage, Seth Hampson, and Blaise Aguera y Arcas. Communication-efficient learning of deep networks from decentralized data. In *Artificial intelligence and statistics*, pages 1273–1282. PMLR, 2017. 1, 3, 6

[28] Gergely Dánél Németh, Miguel Angel Lozano, Novi Quadrianto, and Nuria M Oliver. A snapshot of the frontiers of client selection in federated learning. *Transactions on Machine Learning Research*, 2022. 2

[29] Alina Oprea and Apostol Vassilev. Adversarial machine learning: A taxonomy and terminology of attacks and mitigations. Technical report, National Institute of Standards and Technology US Department of Commerce, 2023. 2

[30] Adam Paszke, Sam Gross, Soumith Chintala, Gregory Chanan, Edward Yang, Zachary DeVito, Zeming Lin, Alban Desmaison, Luca Antiga, and Adam Lerer. Automatic differentiation in pytorch. In *NIPS 2017 Workshop Autodiff Submission*, 2017. 7

[31] Yuxin Shi, Han Yu, and Cyril Leung. Towards fairness-aware federated learning. *IEEE Transactions on Neural Networks and Learning Systems*, 2023. 9

[32] MyungJae Shin, Chihoon Hwang, Joongheon Kim, Jihong Park, Mehdi Bennis, and Seong-Lyun Kim. Xor mixup: Privacy-preserving data augmentation for one-shot federated learning. *arXiv preprint arXiv:2006.05148*, 2020. 1, 2

[33] Reza Shokri, Marco Stronati, Congzheng Song, and Vitaly Shmatikov. Membership inference attacks against machine learning models. In *2017 IEEE symposium on security and privacy (SP)*, pages 3–18. IEEE, 2017. 2

[34] Liwei Song, Reza Shokri, and Prateek Mittal. Membership inference attacks against adversarially robust deep learning models. In *2019 IEEE Security and Privacy Workshops (SPW)*, pages 50–56. IEEE, 2019. 2

[35] Nitish Srivastava, Geoffrey Hinton, Alex Krizhevsky, Ilya Sutskever, and Ruslan Salakhutdinov. Dropout: a simple way to prevent neural networks from overfitting. *The journal of machine learning research*, 15(1):1929–1958, 2014. 5

[36] Jasper Tan, Daniel LeJeune, Blake Mason, Hamid Javadi, and Richard G Baraniuk. A blessing of dimensionality in membership inference through regularization. In *International Conference on Artificial Intelligence and Statistics*, pages 10968–10993. PMLR, 2023. 2

[37] Jie Xu, Benjamin S Glicksberg, Chang Su, Peter Walker, Jiang Bian, and Fei Wang. Federated learning for healthcare informatics. *Journal of Healthcare Informatics Research*, 5: 1–19, 2021. 1

[38] Lixuan Yang, Cedric Beliard, and Dario Rossi. Heterogeneous data-aware federated learning. *IJCAI 2020 Federated Learning Workshop*, 2020. 7

[39] Samuel Yeom, Irene Giacomelli, Matt Fredrikson, and Somesh Jha. Privacy risk in machine learning: Analyzing the connection to overfitting. In *2018 IEEE 31st computer se-*

curity foundations symposium (CSF), pages 268–282. IEEE, 2018. 2, 3, 6

[40] Chan Yun-Hin, Jiang Zhihan, Deng Jing, and Ngai C-H Edith. Fedin: Federated intermediate layers learning for model heterogeneity. *arXiv preprint arXiv:2304.00759*, 2023. 2

[41] Chi Zhang, Zhang Xiaoman, Ekanut Sotthiwat, Yanyu Xu, Ping Liu, Liangli Zhen, and Yong Liu. Generative gradient inversion via over-parameterized networks in federated learning. In *Proceedings of the IEEE/CVF International Conference on Computer Vision*, pages 5126–5135, 2023. 2

[42] Wei Zhang, Jun Tanida, Kazuyoshi Itoh, and Yoshiki Ichioka. Shift-invariant pattern recognition neural network and its optical architecture. In *Proceedings of annual conference of the Japan Society of Applied Physics*. Montreal, CA, 1988. 5

Addressing Membership Inference Attack in Federated Learning with Model Compression

Supplementary Material

7. Machine learning model description

The model in all our experiments is a Convolutional Neural Network, similar to the models reported in related work [3]. The layers with weight matrices consist of 2D convolutional layers with a (N, M, H, W) 4-dimensional matrix, where the first two dimensions N and M correspond the output and input channels and the rest are the convolutional kernels. From a model-agnostic perspective, N and M are the dimensions that change when the clients in the federation learn models of different size than the server's model whereas H and W are the same as in the server. In the PyTorch implementation, the bias of the convolutional layers has a separate (N) 1-dimensional matrix. When a subset of N_c^l output channels is selected for a client c and convolutional layer l , its bias shares the same N_c^l out of N^l output channels.

After the convolutional layers in the model architecture, there are BatchNorm normalization layers with (N) 1-dimensional weight matrices with bias. Note that the BatchNorm layer $l + 2$ after convolutional layer l has the same $N_c^{l+2} = N_c^l$ channels selected. The Scaler layer adapted from HeteroFL [3] scales its input with respect to the model-agnostic compression rate. For $r_c = \frac{N_c}{N} = \frac{M_c}{M}$, the Scaler follows:

$$f_{\text{Scaler}}(x) = \frac{1}{r_c}x. \quad (9)$$

Finally, there is a linear layer l with weight matrix (N, M) and bias with weight matrix size (N) . Each client c shares the same N_c^l output channels on this linear layer.

The complexity of the model is controlled with parameter u . Each input and output dimension of the weight matrix is a multiple of u . The model complexity levels used in this paper –namely 30k, 100k, 400k, and 1.6M– correspond to u values of 8, 16, 32, and 64, respectively. Figure 5 illustrates the model architecture for a generic u and an example with $u = 16$.

8. Detailed experimental results

8.1. Model size vs attack advantage

Tab. 3 shows the Pearson correlation coefficient between the client dataset sizes and their vulnerability against client-side Yeom membership inference attacks. Numbers correspond to running experiments 5 times in a federation with 10 clients. Clients with less than 400 data samples are excluded from the analysis, resulting in the exclusion of 3

Fix model architecture		Changing size			
		u=16		u	
Input (32x32x3)	(HxW)	N	M	N	M
Conv2D	3x3	16	3	u	3
Scaler					
BatchNorm		16		u	
ReLU					
MaxPool2D					
Conv2D	3x3	32	16	2u	u
Scaler					
BatchNorm		32		2u	
ReLU					
MaxPool2D					
Conv2D	3x3	64	32	4u	2u
Scaler					
BatchNorm		64		4u	
ReLU					
MaxPool2D					
Conv2D	3x3	128	64	8u	4u
Scaler					
BatchNorm		128		8u	
ReLU					
GlobalAveragePool2D					
Flatten					
Dense		10	128	10	8u
Output (10)					

Figure 5. Model architecture and sizes of the weight matrices depending on the model complexity, controlled by the parameter u . Layer names and constant parameter dimensions on the left, varying dimensions on the right.

clients in the 5 runs with the CIFAR-10 and CIFAR-100 datasets. All values in the table exceed the critical value of non-significant correlation for the given sample size.

8.2. Server and client side results for different model agnostic methods

Tab. 4 shows the results summarized in Fig. 3 of the main part of the manuscript. Tab. 5 contains the results illustrated in Fig. 4. Experiments are repeated 3 times, with both the average and standard deviation reported. As depicted in Fig. 3, Fig. 4 and the tables, the models learned with

# Model parameters	30k	100k	400k	1.6M
CIFAR-10	-0.62	-0.65	-0.57	-0.87
CIFAR-100	-0.54	-0.70	-0.85	-0.90
FEMNIST	-0.71	-0.65	-0.63	-0.75

Table 3. Pearson correlation coefficient of dataset size and attack advantage for different model sizes in class-balanced heterogeneous data distribution.

MaPP-FL have the best accuracy-privacy trade-off in the clients while maintaining competitive results in the server.

9. Input-output channel dependency

In Sec. 4.2 we present FDropout [3] and HeteroFL [1] according to their original descriptions, which suggest that the channels of a layer l can be dropped independently from the previous and following channels. However, after extensive experiments, we observed that the client models train significantly better if the selected output channels of a convolutional layer are *the same* as the input channels of the following convolutional layer. In the FDropout adaptation of [4] the same principled is adopted: layer l only drops output channels randomly, while the selection of the input channels is inherited from the previous convolutional layer. The pseudo-code in [2] suggests that their implementation follows the original layer-independent dropout and their results show that FDropout performs badly compared to other techniques: while the Simple Ensemble Averaging method reached the 70% accuracy of the baseline FedAvg on FEMNIST dataset, the presented implementation of FDropout only reached 60%. In Tab. 6, we compare FDropout and MaPP-FL (R) with input and output channels dropped independently and with layer-wise coupling with respect to the previous and following layer. The results show that the client side accuracy for the layer-wise methods outperforms their independent counterpart by 16% for FDropout and 7% for MaPP-FL. Based on these results we conclude that the layer-wise dependency is necessary to achieve competitive results and follow this principle in our other experiments.

Additionally, Section 7 in this supplementary material describes how the BatchNorm layers in our implementation have the same channels dropped as the previous convolutional layers.

10. MaPP-FL

Algorithm 1 contains the pseudo-code description of the MaPP-FL channel selection algorithm.

11. Zero large clients

Note that Tab. 4 includes a special case when 0 clients have the same model size as the server's. Regarding HeteroFL,

Algorithm 1 MaPP-FL

Example with four groups.

```

1: Initialize the groups:
2: if variation  $M$  then
3:   Set the channels of the 4 groups following the sub-
   matrix structure: first or second half of channels in each
   layer.
4: else (variation  $R$ )
5:   Select the set of channels randomly.
6: end if
7: for  $t = 1..T$  do
8:   Randomly put clients into the groups.
9:   Select init weights for  $\theta_c^t$  following the group's rule.
10:  Client trains the reduced models to get  $\theta_c^t$ .
11:  Server maps back the weights to their position in
     $\theta^t$ .
12:  Server aggregates the weights to get  $\theta^{t+1}$ 
13: end for
14: Server uses model  $\theta^{T+1}$ 
15: Clients use the model  $\theta_c^T$  that fits into their memory.

```

this is equivalent to training a smaller sized server model using FedAvg while the remaining weights in the server's model are the same as those at initialization. Thus, the server and average client side accuracies are approximately the same. In the case of MaPP-FL (M), the server side accuracy is worse than that of FedAvg while the average client side accuracy remains competitive. The reason behind this is that in the sub-matrix variation of MaPP-FL the client groups select disjoint channel sets. Thus, in the case of 4 groups of small clients, each of the groups learns an independent model and the only aggregation takes place in the server. Thus, the FL architecture does not yield a competitive server model.

References

- [1] Sebastian Caldas, Jakub Konečny, H. Brendan McMahan, and Ameet Talwalkar. Expanding the reach of federated learning by reducing client resource requirements, 2018
- [2] Gary Cheng, Zachary Charles, Zachary Garrett, and Keith Rush. Does federated dropout actually work? In *Proceedings of the IEEE/CVF Conference on Computer Vision and Pattern Recognition*, pages 3387–3395, 2022.
- [3] Enmao Diao, Jie Ding, and Vahid Tarokh. Hetero{fl}: Computation and communication efficient federated learning for heterogeneous clients. In *International Conference on Learning Representations*, 2021.
- [4] Dongping Liao, Xitong Gao, Yiren Zhao, and Cheng-Zhong Xu. Adaptive channel sparsity for federated learning under system heterogeneity. In *Proceedings of the IEEE/CVF Conference on Computer Vision and Pattern Recognition*, pages 20432–20441, 2023

#	Server side						Average client side					
	FDropout		HeteroFL		MaPP-FL		FDropout		HeteroFL		MaPP-FL	
	Acc↑	Adv↓	Acc↑	Adv↓	Acc↑	Adv↓	Acc↑	Adv↓	Acc↑	Adv↓	Acc↑	Adv↓
0	59.22 σ 0.65	0.53 σ 1.54	70.43 σ 0.91	1.91 σ 0.88	44.03 σ 2.04	0.67 σ 0.89	37.74 σ 0.64	1.80 σ 0.63	70.31 σ 0.57	2.98 σ 0.79	69.42 σ 0.27	2.91 σ 0.17
1	73.95 σ 2.13	1.78 σ 0.55	75.32 σ 2.10	3.77 σ 1.29	76.32 σ 1.44	2.64 σ 0.68	41.23 σ 1.60	2.46 σ 0.54	69.25 σ 0.66	3.40 σ 1.23	69.42 σ 1.04	3.07 σ 0.67
2	76.30 σ 1.18	2.44 σ 0.76	77.86 σ 1.57	3.77 σ 0.83	77.66 σ 0.97	3.01 σ 1.09	40.68 σ 1.71	2.84 σ 0.63	68.75 σ 0.65	3.64 σ 0.89	68.02 σ 1.17	3.38 σ 0.81
3	77.98 σ 0.39	2.67 σ 0.82	78.38 σ 0.77	3.55 σ 1.46	78.26 σ 0.81	3.05 σ 1.32	44.11 σ 1.89	2.94 σ 0.67	70.11 σ 0.74	3.96 σ 0.95	68.04 σ 0.93	3.15 σ 0.96
4	78.57 σ 0.80	3.13 σ 0.79	78.92 σ 0.59	3.39 σ 0.28	78.36 σ 0.39	3.01 σ 0.42	45.37 σ 1.52	2.96 σ 0.50	71.09 σ 0.72	4.49 σ 0.96	68.25 σ 0.51	3.32 σ 0.36
5	78.11 σ 0.44	3.54 σ 0.43	79.02 σ 0.20	2.95 σ 0.48	79.12 σ 0.38	2.52 σ 1.28	52.07 σ 0.72	2.97 σ 1.08	70.74 σ 0.80	4.38 σ 0.79	68.95 σ 0.81	3.26 σ 0.81
6	79.31 σ 0.10	3.27 σ 0.70	78.75 σ 0.35	3.99 σ 1.25	78.59 σ 1.21	2.75 σ 0.51	56.72 σ 0.15	3.47 σ 0.74	72.09 σ 0.101	5.02 σ 0.84	68.67 σ 1.05	4.13 σ 0.29
7	78.98 σ 0.70	3.72 σ 1.02	79.11 σ 0.39	3.50 σ 0.53	78.52 σ 0.31	2.85 σ 0.56	62.58 σ 1.14	4.35 σ 0.31	73.43 σ 0.91	5.33 σ 0.18	69.72 σ 0.85	4.23 σ 0.94
8	79.26 σ 0.62	3.59 σ 0.63	78.93 σ 0.59	3.33 σ 0.20	78.89 σ 0.01	3.56 σ 0.81	67.55 σ 0.22	4.17 σ 0.42	73.68 σ 0.25	5.56 σ 0.53	71.16 σ 0.12	4.48 σ 0.18
9	79.06 σ 0.89	3.19 σ 1.36	79.07 σ 0.22	2.78 σ 0.90	78.33 σ 0.18	3.26 σ 1.30	73.22 σ 0.83	4.29 σ 0.74	74.77 σ 1.26	5.05 σ 0.73	72.93 σ 0.46	4.53 σ 0.59

(a) CIFAR10

#	Server side						Average client side					
	FDropout		HeteroFL		MaPP-FL		FDropout		HeteroFL		MaPP-FL	
	Acc↑	Adv↓	Acc↑	Adv↓	Acc↑	Adv↓	Acc↑	Adv↓	Acc↑	Adv↓	Acc↑	Adv↓
0	22.61 σ 0.71	-0.16 σ 1.14	34.71 σ 0.62	0.10 σ 0.33	10.62 σ 1.19	-0.45 σ 0.85	8.89 σ 0.20	1.25 σ 0.46	34.78 σ 0.41	2.86 σ 0.61	32.74 σ 0.40	2.84 σ 0.49
1	36.66 σ 2.63	0.86 σ 1.07	39.19 σ 4.58	3.41 σ 0.37	41.03 σ 3.12	2.45 σ 0.98	10.94 σ 1.08	2.14 σ 0.43	32.66 σ 0.67	4.95 σ 0.04	32.22 σ 0.32	3.79 σ 0.42
2	42.32 σ 2.12	1.63 σ 0.67	43.86 σ 2.19	3.33 σ 0.92	42.50 σ 1.97	1.87 σ 0.87	12.99 σ 0.77	2.40 σ 0.37	32.65 σ 0.67	5.82 σ 0.34	31.43 σ 1.21	3.77 σ 0.53
3	43.21 σ 1.65	1.64 σ 0.73	45.15 σ 1.56	2.59 σ 0.13	44.62 σ 1.40	2.43 σ 0.23	16.16 σ 0.34	2.84 σ 0.73	34.08 σ 1.25	6.18 σ 0.40	31.63 σ 0.64	4.32 σ 0.27
4	44.42 σ 1.24	2.13 σ 0.49	45.52 σ 1.73	2.99 σ 0.86	44.48 σ 0.68	1.61 σ 0.61	20.23 σ 0.12	3.54 σ 1.10	35.00 σ 0.81	6.27 σ 0.92	32.31 σ 0.45	4.58 σ 0.41
5	45.20 σ 1.45	2.55 σ 0.34	46.13 σ 0.41	2.38 σ 0.65	45.92 σ 0.57	2.15 σ 0.85	24.48 σ 0.50	4.47 σ 0.53	36.57 σ 0.95	6.16 σ 0.63	32.89 σ 0.58	5.15 σ 0.29
6	45.59 σ 0.64	3.16 σ 0.39	45.81 σ 0.31	2.96 σ 0.89	45.53 σ 0.83	2.41 σ 0.76	28.53 σ 0.61	4.81 σ 0.24	37.52 σ 0.54	6.63 σ 0.32	34.23 σ 0.60	5.40 σ 0.09
7	46.47 σ 0.90	2.56 σ 0.42	45.61 σ 1.07	2.33 σ 0.64	45.31 σ 0.33	3.01 σ 0.18	33.69 σ 0.71	5.14 σ 0.11	38.61 σ 1.03	6.64 σ 0.55	35.46 σ 0.24	5.59 σ 0.83
8	46.17 σ 0.52	2.03 σ 1.13	46.04 σ 0.63	1.96 σ 1.24	45.40 σ 0.48	2.49 σ 0.50	37.76 σ 0.61	6.21 σ 0.75	40.30 σ 0.37	6.99 σ 1.22	38.10 σ 0.68	6.18 σ 0.10
9	45.95 σ 1.20	2.60 σ 0.23	46.30 σ 0.16	2.08 σ 0.30	45.61 σ 0.40	2.52 σ 0.23	41.70 σ 0.77	6.03 σ 1.15	42.18 σ 0.40	7.47 σ 0.62	41.49 σ 0.24	6.52 σ 1.25

(b) CIFAR100

#	Server side						Average client side					
	FDropout		HeteroFL		MaPP-FL		FDropout		HeteroFL		MaPP-FL	
	Acc↑	Adv↓	Acc↑	Adv↓	Acc↑	Adv↓	Acc↑	Adv↓	Acc↑	Adv↓	Acc↑	Adv↓
0	79.83 σ 0.43	2.29 σ 0.23	85.37 σ 0.53	5.59 σ 0.46	31.30 σ 4.49	2.83 σ 1.22	41.82 σ 3.06	8.32 σ 0.54	85.29 σ 0.73	10.00 σ 0.72	84.42 σ 0.13	9.56 σ 0.51
1	84.68 σ 0.23	2.81 σ 0.69	80.55 σ 1.17	4.43 σ 1.59	83.25 σ 0.26	4.73 σ 0.66	48.12 σ 2.14	8.24 σ 0.71	83.78 σ 0.25	12.61 σ 1.08	82.88 σ 0.34	11.00 σ 0.22
2	85.49 σ 0.92	3.69 σ 0.68	82.73 σ 0.54	6.13 σ 1.23	85.49 σ 0.46	5.47 σ 0.42	47.63 σ 1.88	9.08 σ 0.69	83.08 σ 0.21	13.61 σ 0.54	82.67 σ 0.29	11.34 σ 0.75
3	85.60 σ 0.34	5.57 σ 0.28	84.16 σ 0.61	6.95 σ 0.54	85.68 σ 0.22	6.45 σ 1.05	47.04 σ 1.95	10.34 σ 0.85	82.83 σ 0.47	14.54 σ 0.67	81.72 σ 0.50	12.02 σ 1.03
4	86.32 σ 0.12	5.91 σ 0.80	84.95 σ 0.33	8.68 σ 0.57	86.60 σ 0.42	7.10 σ 0.20	48.46 σ 0.34	10.76 σ 0.36	83.26 σ 0.11	14.63 σ 0.65	81.88 σ 0.14	12.71 σ 0.27
5	86.42 σ 0.32	7.75 σ 0.56	85.28 σ 0.31	8.87 σ 0.67	86.22 σ 0.36	7.75 σ 0.59	54.12 σ 1.02	11.25 σ 0.45	82.87 σ 0.36	15.27 σ 0.65	80.77 σ 0.35	13.47 σ 0.36
6	86.85 σ 0.03	8.31 σ 0.75	86.22 σ 0.29	9.49 σ 1.35	86.50 σ 0.16	8.45 σ 0.18	58.52 σ 0.89	11.47 σ 0.56	83.15 σ 0.21	16.07 σ 0.13	80.38 σ 0.34	13.83 σ 0.81
7	86.89 σ 0.30	9.34 σ 0.66	86.59 σ 0.44	9.17 σ 0.41	86.97 σ 0.07	8.51 σ 0.39	66.02 σ 0.07	12.86 σ 0.12	83.40 σ 0.34	16.03 σ 0.49	80.46 σ 0.46	13.82 σ 0.39
8	86.43 σ 0.32	9.21 σ 0.37	86.26 σ 0.48	8.99 σ 0.48	86.67 σ 0.42	9.05 σ 0.21	71.44 σ 0.27	12.54 σ 0.39	83.42 σ 0.39	16.19 σ 0.52	80.06 σ 0.72	13.45 σ 0.46
9	86.55 σ 0.57	8.83 σ 0.48	86.84 σ 0.62	8.91 σ 0.54	86.76 σ 0.25	8.91 σ 0.63	78.82 σ 0.67	12.50 σ 0.62	84.14 σ 1.13	15.46 σ 1.27	81.18 σ 0.41	13.37 σ 0.27

(c) FEMNIST

Table 4. Detailed experimental results for Fig. 3

Name	Server		Client average	
	Acc↑	Adv↓	Acc↑	Adv↓
FedAvg(100k)	78.17 σ 0.37	2.03 σ 0.51	76.64 σ 0.56	4.53 σ 0.23
FedAvg(30k)	69.23 σ 0.49	0.78 σ 0.51	67.66 σ 0.28	2.65 σ 0.6
Local	-	-	52.52 σ 0.62	-
OSR	76.69 σ 0.37	1.64 σ 0.08	30.64 σ 1.74	1.62 σ 0.88
OSM	78.05 σ 0.58	2.04 σ 0.42	59.63 σ 1.44	2.85 σ 0.19
HeteroFL (R) : OFR	78.13 σ 0.52	2.94 σ 0.45	69.73 σ 0.64	4.12 σ 0.07
HeteroFL: OFM	78.26 σ 0.78	2.51 σ 0.53	69.76 σ 0.34	3.80 σ 0.34
GSR	76.11 σ 0.03	2.11 σ 0.35	40.07 σ 2.58	1.81 σ 0.18
MaPP-FL (M) : GFM	77.00 σ 0.41	1.49 σ 0.06	68.26 σ 0.48	2.99 σ 0.36
MaPP-FL (R) : GFR	77.72 σ 0.24	1.83 σ 0.77	67.62 σ 0.82	2.60 σ 0.45
UFR	77.59 σ 0.86	1.01 σ 0.6	63.33 σ 0.44	2.54 σ 0.34
FDropout: USR	76.42 σ 0.18	1.9 σ 0.52	42.06 σ 0.69	2.05 σ 0.70

Table 5. Ablation study of different channel selection methods for model agnostic Federated Learning. CIFAR-10 dataset, class-balanced distribution, 2 large clients. Repeated 3 times with the same dataset size distribution between repeats

Name	Server		Client average	
	Acc↑	Adv↓	Acc↑	Adv↓
FDropout independent	75.44 σ 1.75	2.57 σ 1.62	23.56 σ 0.29	1.74 σ 0.44
FDropout layerwise	76.38 σ 1.36	2.45 σ 1.34	39.99 σ 1.11	2.32 σ 1.52
MaPP-FL (R) independent	76.41 σ 1.73	2.87 σ 0.78	55.82 σ 1.61	3.00 σ 0.50
MaPP-FL (R) layerwise	77.11 σ 1.52	3.34 σ 0.98	62.80 σ 1.43	3.20 σ 0.24

Table 6. Input-output channels selected independently and with respect to the previous layers in the model. FDropout and MaPP-FL (R) experiments on CIFAR-10 with 2 large clients out of 10 clients in total, repeated 3 times. Client-side performance is significantly better when the channel selection is structured layerwise compared to their independent counterparts.